



OPEN

Reduced B7-H3 expression by *PAX3-FOXO1* knockdown inhibits cellular motility and promotes myogenic differentiation in alveolar rhabdomyosarcoma

Takuyo Kanayama, Mitsuru Miyachi✉, Yohei Sugimoto, Shigeki Yagyū, Ken Kikuchi, Kunihiro Tsuchiya, Tomoko Iehara & Hajime Hosoi

B7-H3 (also known as CD276) is associated with aggressive characteristics in various cancers. Meanwhile, in alveolar rhabdomyosarcoma (ARMS), *PAX3-FOXO1* fusion protein is associated with increased aggressiveness and poor prognosis. In the present study, we explored the relationship between *PAX3-FOXO1* and B7-H3 and the biological roles of B7-H3 in ARMS. Quantitative real time PCR and flow cytometry revealed that *PAX3-FOXO1* knockdown downregulated B7-H3 expression in all the selected cell lines (Rh-30, Rh-41, and Rh-28), suggesting that *PAX3-FOXO1* positively regulates B7-H3 expression. Gene expression analysis revealed that various genes and pathways involved in chemotaxis, INF- γ production, and myogenic differentiation were commonly affected by the knockdown of *PAX3-FOXO1* and *B7-H3*. Wound healing and transwell migration assays revealed that both *PAX3-FOXO1* and *B7-H3* were associated with cell migration. Furthermore, knockdown of *PAX3-FOXO1* or *B7-H3* induced myogenin expression in all cell lines, although myosin heavy chain induction varied depending on the cellular context. Our results indicate that *PAX3-FOXO1* regulates B7-H3 expression and that *PAX3-FOXO1* and B7-H3 are commonly associated with multiple pathways related to an aggressive phenotype in ARMS, such as cell migration and myogenic differentiation block.

Abbreviations

ARMS	Alveolar rhabdomyosarcoma
CAR	Chimeric antigen receptor
ERMS	Embryonal rhabdomyosarcoma
GSEA	Gene set enrichment analysis
qRT-PCR	Quantitative real time polymerase chain reaction
RMS	Rhabdomyosarcoma
siB7-H3	SiRNA targeting <i>B7-H3</i>
siCont	Control siRNA
siPF	SiRNA targeting <i>PAX3-FOXO1</i>

Background

B7-H3 (also known as CD276), a member of the B7 family of type I transmembrane proteins, is known to modulate T-cell function in a costimulatory^{1,2} or coinhibitory^{3,4} manner. Although B7-H3 protein has limited expression in normal human tissues, it is broadly overexpressed in various human cancers⁵⁻⁹, including

Department of Pediatrics, Graduate School of Medical Science, Kyoto Prefectural University of Medicine, 465, Kajii-cho, Kawaramachi-Hirokoji, Kamigyo-ku, Kyoto 602-8566, Japan. ✉email: mmiyachi@koto.kpu-m.ac.jp

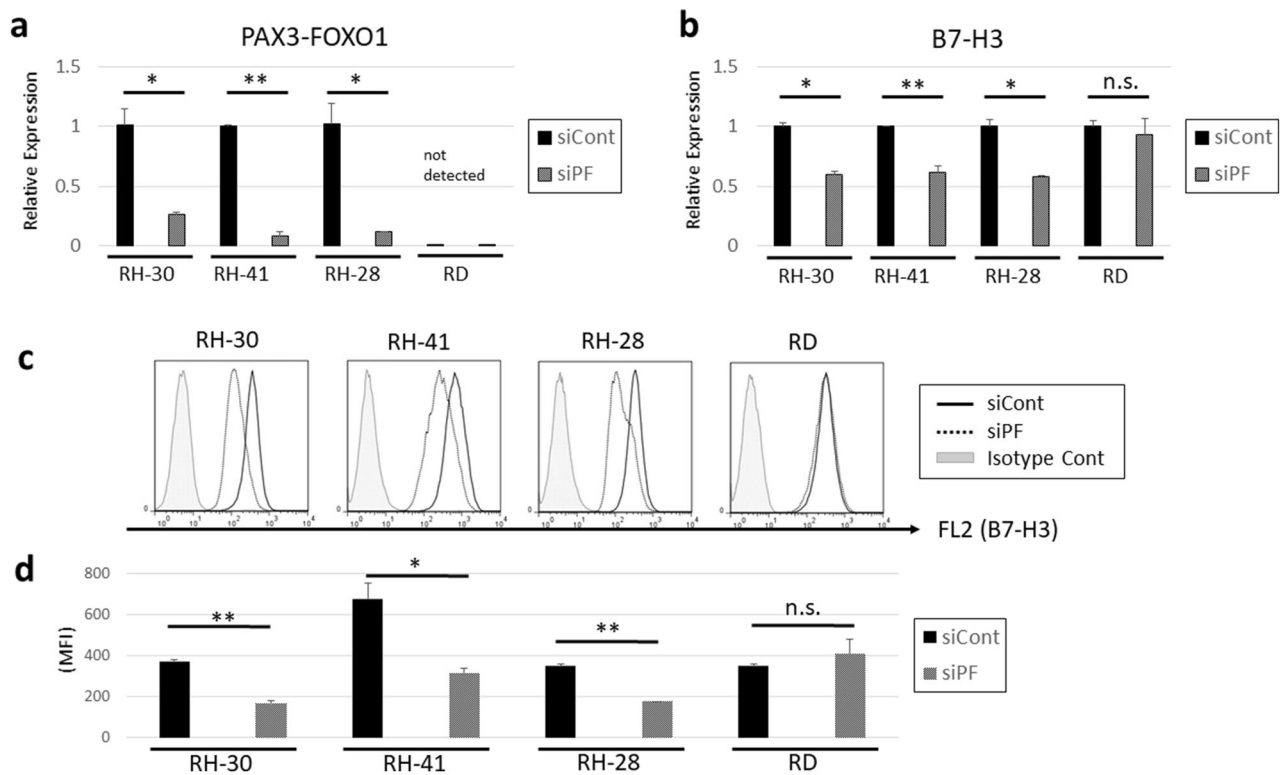


Figure 1. Knockdown of *PAX3-FOXO1* downregulates the expression of *B7-H3*. (a) Quantitative real-time PCR (qRT-PCR) analysis of *PAX3-FOXO1*. Knockdown efficacy of *PAX3-FOXO1* was confirmed in three *PAX3-FOXO1* positive ARMS cell lines. RD, a *PAX3-FOXO1*-negative cell line, was used as a negative control. (b) qRT-PCR analysis of *B7-H3*. (c) Representative histogram of flow cytometry analysis of *B7-H3*. (d) Mean fluorescence index of *B7-H3* in flow cytometry analysis. Results shown are means \pm SD. * $p < 0.05$, ** $p < 0.01$, n.s. $p > 0.05$, by two-tailed unpaired t test.

rhabdomyosarcoma¹⁰. Therefore, B7-H3 has been highlighted in recent years as an attractive surface antigen for molecular targeted therapy, such as those using monoclonal antibody¹¹ and chimeric antigen receptor (CAR) T-cells^{10,12}. In addition to its immune regulatory roles in the tumor microenvironment, B7-H3 is known to be associated with tumor cell proliferation, migration, invasion, metabolism, and angiogenesis; therefore, it is related to a poor prognosis^{13–19}.

Rhabdomyosarcoma (RMS) is the most common soft tissue malignancy in children²⁰. It consists of two major subtypes, namely the alveolar RMS (ARMS) and the embryonal RMS (ERMS). The majority of ARMS are associated with specific fusion proteins, *PAX3-FOXO1* or *PAX7-FOXO1*^{21–23}. The expression of *PAX3-FOXO1* is associated with increased aggressiveness and a poor prognosis²⁴. *PAX3-FOXO1* may function as a more potent transcriptional activator than *PAX3*, and induces the expression of a number of transcriptional targets that lead to tumorigenesis, cell proliferation, migration, invasion, and differentiation block^{25–27}.

Although *PAX3-FOXO1* contributes to aggressive characteristics in ARMS, and B7-H3 does the same in other cancers, limited information is available regarding the function of B7-H3 in ARMS and about the relationship between *PAX3-FOXO1* and B7-H3. In this context, we hypothesized that *PAX3-FOXO1* regulates B7-H3 expression and contributes to aggressive characteristics in ARMS. In this study, we analyzed the association of *PAX3-FOXO1* and B7-H3 by knocking down the expression of *PAX3-FOXO1* and performing gene expression analysis. We demonstrate that *PAX3-FOXO1* knockdown downregulates the expression of B7-H3 in ARMS and that *PAX3-FOXO1* and B7-H3 share common gene expression profiles, which contribute to the aggressive phenotype of ARMS.

Results

B7-H3 expression is downregulated by *PAX3-FOXO1* knockdown in alveolar rhabdomyosarcoma. To investigate the effect of *PAX3-FOXO1* on the expression of B7-H3, knockdown of *PAX3-FOXO1* transcripts was performed by siRNA targeting *PAX3-FOXO1* (siPF). In each *PAX3-FOXO1* fusion gene-positive ARMS cell line (RH-30, RH-41, and RH-28), a high knockdown efficiency of *PAX3-FOXO1* was confirmed by quantitative real time polymerase chain reaction (qRT-PCR), although *PAX3-FOXO1* was not detected in *PAX3-FOXO1*-negative RD cells (Fig. 1a). Next, qRT-PCR for *B7-H3* revealed that *PAX3-FOXO1* knockdown decreased the expression of *B7-H3* in the *PAX3-FOXO1*-positive cell line, but not in the *PAX3-FOXO1*-negative RD cells (Fig. 1b). In addition, flow cytometry analysis demonstrated that *PAX3-FOXO1* knockdown decreased the expression of B7-H3 in the *PAX3-FOXO1*-positive cell lines, but not in the *PAX3-FOXO1*-negative RD cells

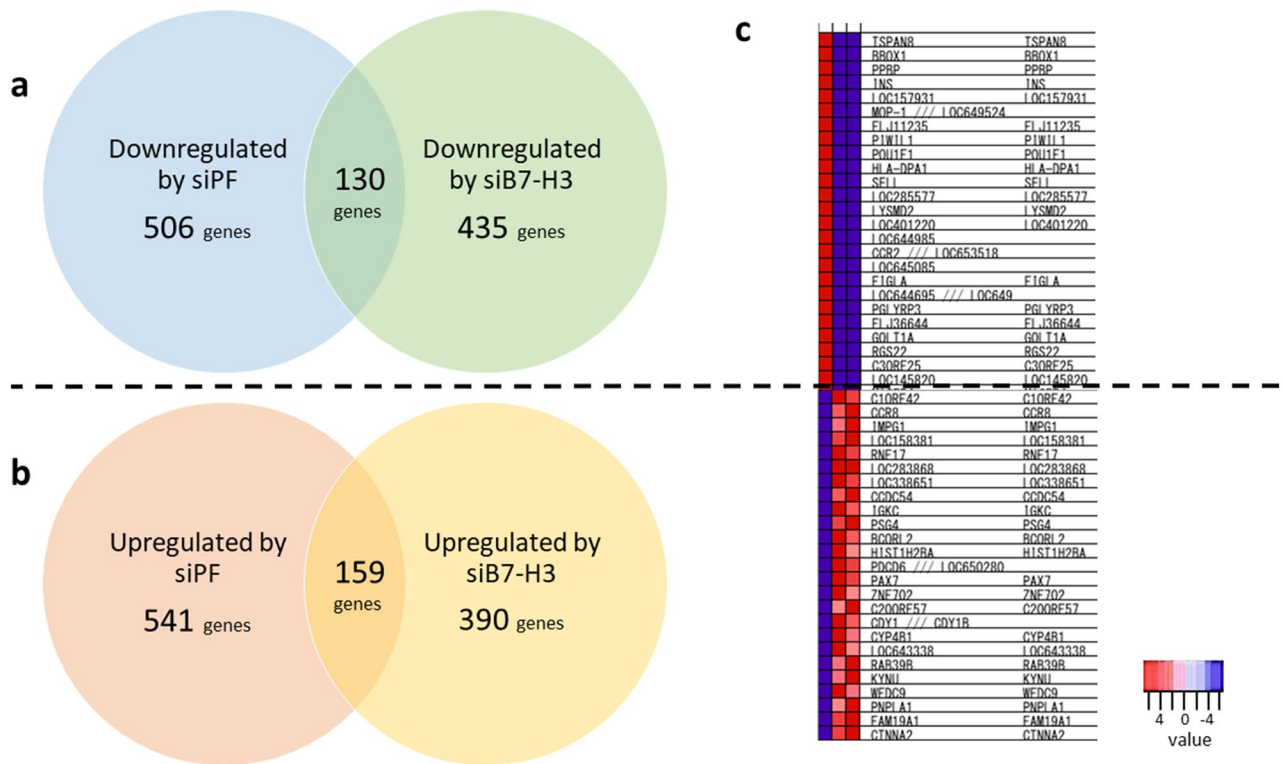


Figure 2. Gene expression analysis. Knockdown of *PAX3-FOXO1* and *B7-H3* reveal shared down/upregulated genes. (a) Venn diagram of genes that were downregulated by the knockdown of *PAX3-FOXO1* or *B7-H3*. (b) Venn diagram of genes that were upregulated by the knockdown of *PAX3-FOXO1* or *B7-H3*. (c) Heat map of the top 50 genes that were down/up-regulated by the knockdown of *PAX3-FOXO1* or *B7-H3*. The left line shows Rh-30 siCont, the middle Rh-30 siPF, and the right siB7-H3.

(Fig. 1c,d). These results suggest that *PAX3-FOXO1* positively regulates the expression of *B7-H3* at both the mRNA and protein levels.

***PAX3-FOXO1* and *B7-H3* are associated with multiple pathways related to an aggressive rhabdomyosarcoma phenotype.** To unravel the pathways affected by *PAX3-FOXO1* and *B7-H3* in ARMS, gene expression analysis was performed using microarray and gene set enrichment analysis (GSEA). The gene expression signature of siPF or siRNA targeting *B7-H3* (siB7-H3) transfected Rh-30 cells (Rh-30 siPF or Rh-30 siB7-H3, respectively) was compared with that of control siRNA (siCont) transfected Rh-30 cells (Rh-30 siCont). Gene expression analysis revealed that in Rh-30 siPF and Rh-30 siB7-H3, the expression levels of 636 and 549 genes were decreased, respectively (\log_2 ratio, ≤ 1.0), and those of 700 and 549 genes were increased, respectively (\log_2 ratio, ≥ 1.0), compared with the respective levels in Rh-30 siCont (Fig. 2a,b). Among them, the expression levels of 130 genes were downregulated and those of 159 genes were upregulated in both the Rh-30 siPF and Rh-30 siB7-H3 compared to the respective levels in the Rh-30 siCont (Fig. 2a,b). A heat map of top 50 shared downregulated or upregulated genes is shown in Fig. 2c.

GSEA revealed that several pathways related to chemotaxis, INF- γ production, and regulation of T cell immunity were inactivated in both Rh-30 siPF and Rh-30 siB7-H3 unlike in Rh30 siCont, suggesting that *PAX3-FOXO1* and *B7-H3* may contribute to tumor cell metastasis and immune evasion (Fig. 3a,b). In contrast, several pathways related to muscle cell differentiation were activated in both Rh-30 siPF and Rh-30 siB7-H3 but not in Rh30 siCont, suggesting that *PAX3-FOXO1* and *B7-H3* may block myoblast differentiation (Fig. 3c,d).

***PAX3-FOXO1* and *B7-H3* are associated with cell migration.** To confirm that *PAX3-FOXO1* and *B7-H3* contribute to metastasis in ARMS, as suggested by GSEA, we performed wound healing and transwell assays. Wound healing assays revealed that cell migration in ARMS was significantly attenuated by the knockdown of *PAX3-FOXO1* or *B7-H3* in all the three cell lines (Fig. 4a,b). The transwell assays similarly demonstrated that cell migration in ARMS was significantly attenuated by the knockdown of *PAX3-FOXO1* or *B7-H3* in all the three cell lines (Fig. 4c).

To determine the pathways contributing to cell migration that are affected by *PAX3-FOXO1* and *B7-H3*, we performed qRT-PCR for *CXCR4* and *STYK1*, as gene expression analysis indicated that both these genes were downregulated in Rh-30 siPF and Rh-30 siB7-H3. As expected, *CXCR4* was downregulated by transfection of all the three cell lines with siPF or siB7-H3 (Fig. 5a). In addition, *STYK1* was downregulated in Rh-30 and Rh-41 by transfection with siPF or siB7-H3, although in Rh28, *STYK1* was downregulated by transfection with siPAX3-FOXO1, but not siB7-H3 (Fig. 5b).

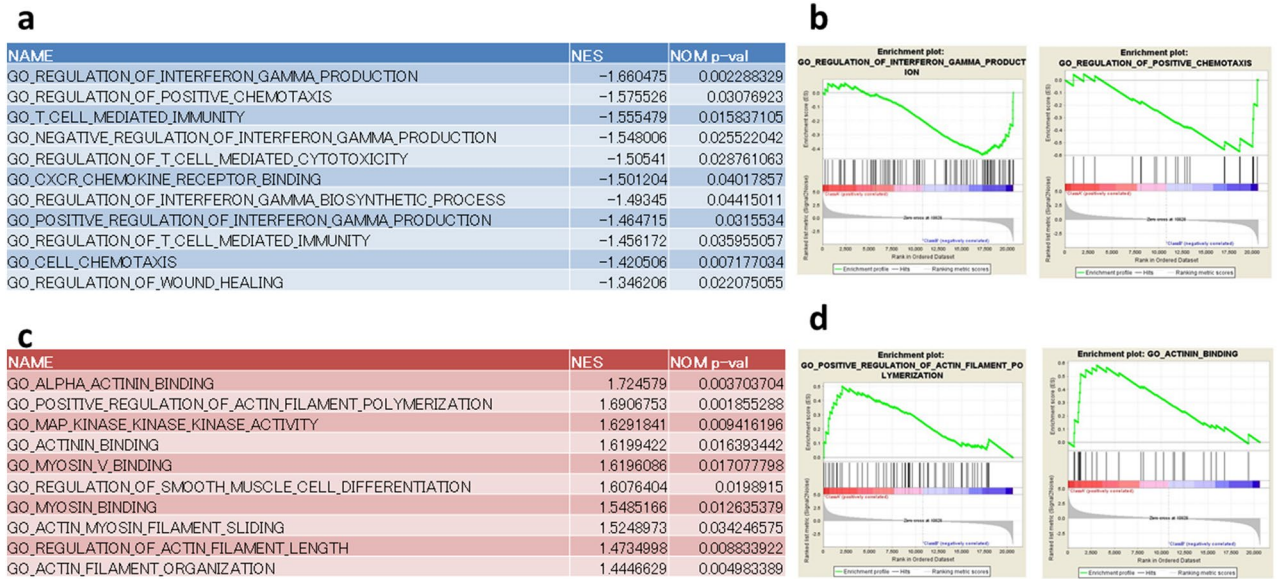


Figure 3. Gene set enrichment analysis (GSEA). **(a)** Representative list of impoverished gene sets upon knockdown of *PAX3-FOXO1* and *B7-H3*. **(b)** Enrichment plot from the GSEA. Interferon gamma production (left panel) and chemotaxis (right panel). **(c)** Representative list of enriched gene sets upon knockdown of *PAX3-FOXO1* and *B7-H3*. **(d)** Enrichment plot from the GSEA. Actin filament polymerization (left panel) and actin binding (right panel).

PAX3-FOXO1 and B7-H3 negatively regulate myogenin expression and interfere with myogenic differentiation. Because the results of GSEA suggested that *PAX3-FOXO1* and *B7-H3* may block myoblast differentiation, we investigated the expression level of myogenin, a transcription factor required for myoblast differentiation, following knockdown of *PAX3-FOXO1* or *B7-H3*. Both qRT-PCR and western blot analyses revealed that myogenin was upregulated in all the three cell lines by transfection with siPF or siB7-H3 (Fig. 6a,b). To investigate whether upregulation of myogenin led to differentiation, we examined the expression level of myosin heavy chain (MyHC) in the ARMS cell lines. Immunofluorescence of MyHC revealed that in Rh-30 cells, transfection with siPF induced MyHC more strongly than the transfection with siB7-H3, whereas in Rh-41 cells, transfection with siB7-H3 induced MyHC more strongly than did siPF (Fig. 6c).

Discussion

In this study, we investigated the regulatory mechanism and function of *B7-H3* in *PAX3-FOXO1*-positive ARMS. *PAX3-FOXO1* regulates the expression of many target genes²⁵, and we determined that *PAX3-FOXO1* also regulates *B7-H3* expression in ARMS. Our data indicate that although regulated by *PAX3-FOXO1*, *B7-H3* regulates the expression of numerous genes, some of which are also regulated by *PAX3-FOXO1*. Therefore, *B7-H3* is considered to be an important protein downstream of *PAX3-FOXO1* that contributes to aggressive characteristics of *PAX3-FOXO1*-positive ARMS.

Based on the GSEA results, we demonstrate that *B7-H3* is associated with cell migration in ARMS, similar to that in various other cancers. However, the mechanisms by which *B7-H3* regulates migration differ according to the type of cancer. For example, *B7-H3* regulates *CXCR4* in gastric cancer¹⁶, PI3K signaling in bladder and colorectal cancers^{14,15}, JAK2-STAT3 signaling in hepatocellular carcinoma²⁸, and MMP-2 in melanoma²⁹. Our data show that *B7-H3* regulates *CXCR4* in ARMS. Notably, *CXCR4* is also regulated by *PAX3-FOXO1*³⁰. Previous reports have shown that antibody to *CXCR4* inhibit metastasis in ARMS³¹. In addition, we found that *PAX3-FOXO1* regulates the expression of *STYK1*, which is also associated with tumor invasion and metastasis^{32,33}, although molecular targeted therapy against *STYK1* is not developed. *B7-H3* also regulates *STYK1* expression in Rh-30 and Rh-41 cells, but not in Rh-28 cells, indicating that the effect of *B7-H3* on *STYK1* varies depending on the ARMS cell line.

Furthermore, we demonstrate that knockdown of *B7-H3*, as well as of *PAX3-FOXO1*, upregulates the expression of myogenin, a transcription factor needed for myogenic differentiation³⁴. Although *PAX3-FOXO1* inhibits myogenic differentiation in ARMS^{26,35}, the effect of *B7-H3* on myogenic differentiation has not been determined. Among the various functions of *B7-H3* in cancer, inhibition of differentiation (not limited to myogenic differentiation) has not been reported. However, despite the observation regarding the induction of myogenin by *B7-H3* knockdown in all three cell lines, the induction of further differentiation as detected by the expression of MyHC was found to vary with the cell line. Knockdown of *PAX3-FOXO1* induced the expression of MyHC more strongly than did the knockdown of *B7-H3* in Rh-30 cells, whereas *B7-H3* knockdown induced the expression of MyHC to a greater extent than did *PAX3-FOXO1* in Rh-41 cells, indicating that myogenin expression, which leads directly to increased expression of MyHC, may be dependent on the cellular context.

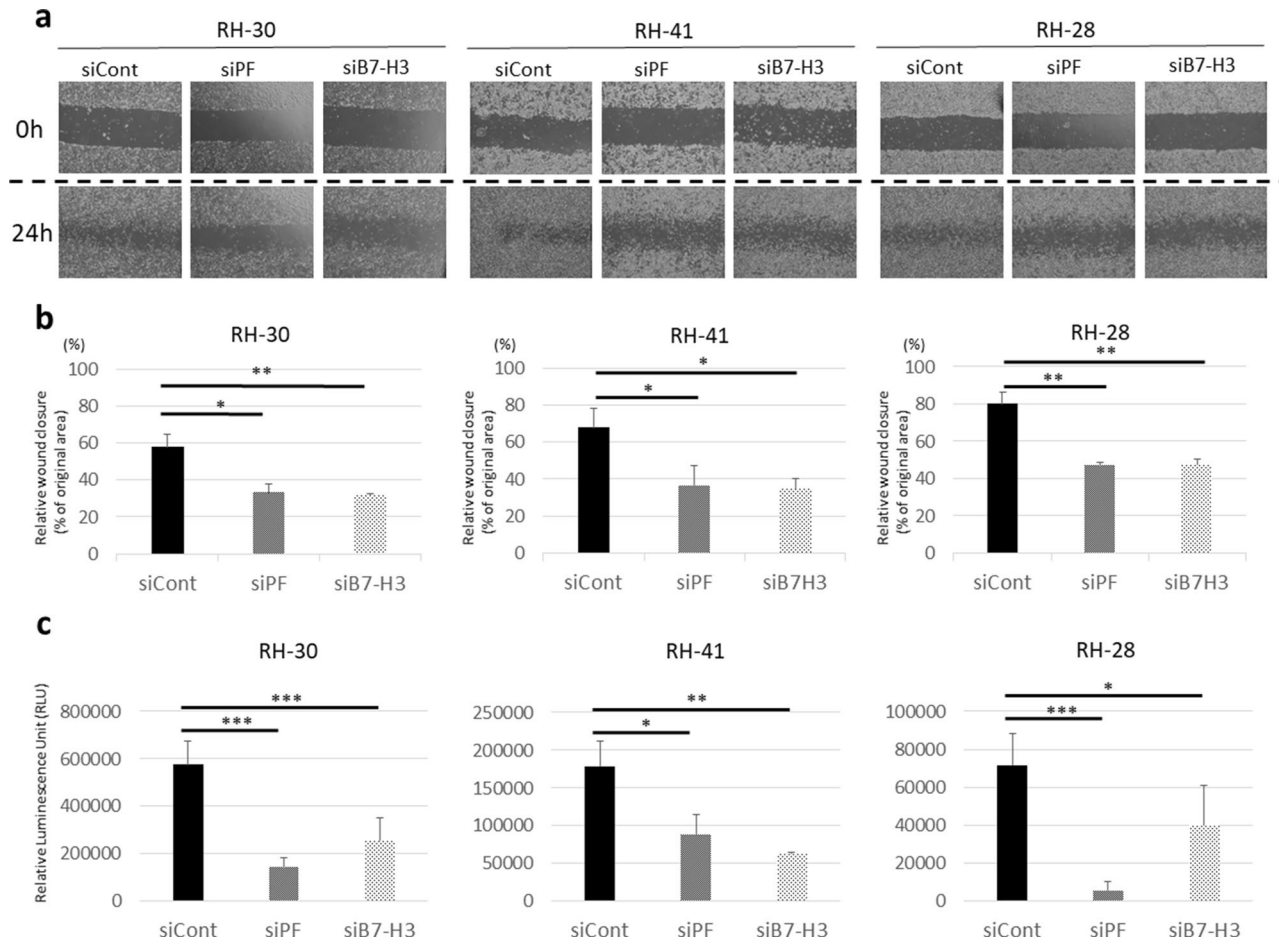


Figure 4. Knockdown of *PAX3-FOXO1* or *B7-H3* attenuates cell migration. **(a)** Representative figure of a wound healing assay. **(b)** Relative healed wound area (% of original wound area) in a wound healing assay. Knockdown of *PAX3-FOXO1* or *B7-H3* attenuates cell migration. **(c)** Transwell assay. Relative luminescence units are shown as the quantification of migratory cells. Results shown are means \pm SD. * $p < 0.05$, ** $p < 0.01$, *** $p < 0.001$, by two-tailed unpaired *t* test.

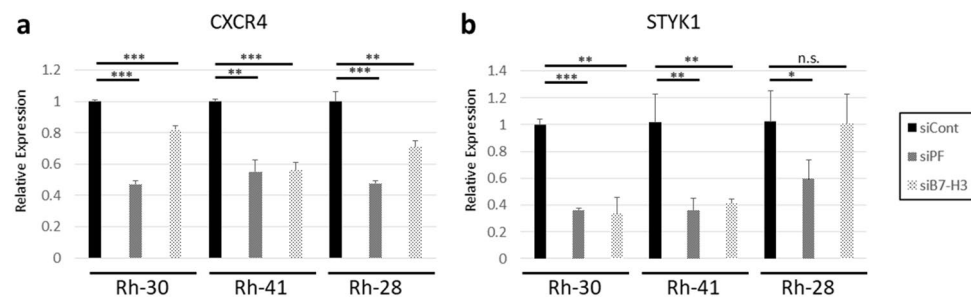


Figure 5. *CXCR4* and *STYK1* expression levels are regulated by *PAX3-FOXO1* and *B7-H3*. **(a)** Quantitative real-time PCR (qRT-PCR) analysis of *CXCR4*. **(b)** qRT-PCR analysis of *STYK1*. Results shown represent means \pm SD. * $p < 0.05$, ** $p < 0.01$, *** $p < 0.001$, n.s. $p > 0.05$, by two-tailed unpaired *t* test.

These results suggest that *B7-H3* might be a potential therapeutic target in ARMS with *PAX3-FOXO1*, which itself is not yet targetable in the present clinical settings. In various cancers, *B7-H3* is an attractive surface antigen for molecular targeted therapy³⁶. Enoblituzumab (MGA271) is a monoclonal antibody for *B7-H3* and causes antibody-dependent cell-mediated cytotoxicity (ADCC)¹¹. Enoblituzumab was evaluated in a phase 1 clinical study and demonstrated acceptable tolerability in the treated patients with solid cancer (trial NCT01391143). Additionally, antibody drug conjugate (ADC) therapies and CAR T cells for *B7-H3* also demonstrated outstanding results in preclinical studies and in a phase 1 clinical trial for childhood cancer^{10,12,37,38}. These targeted therapies for *B7-H3* might be used for treating *PAX3-FOXO1* positive ARMS that exhibits a poor prognosis with conventional intensive therapy. A phase 1 clinical trial of enoblituzumab in children and young adults with

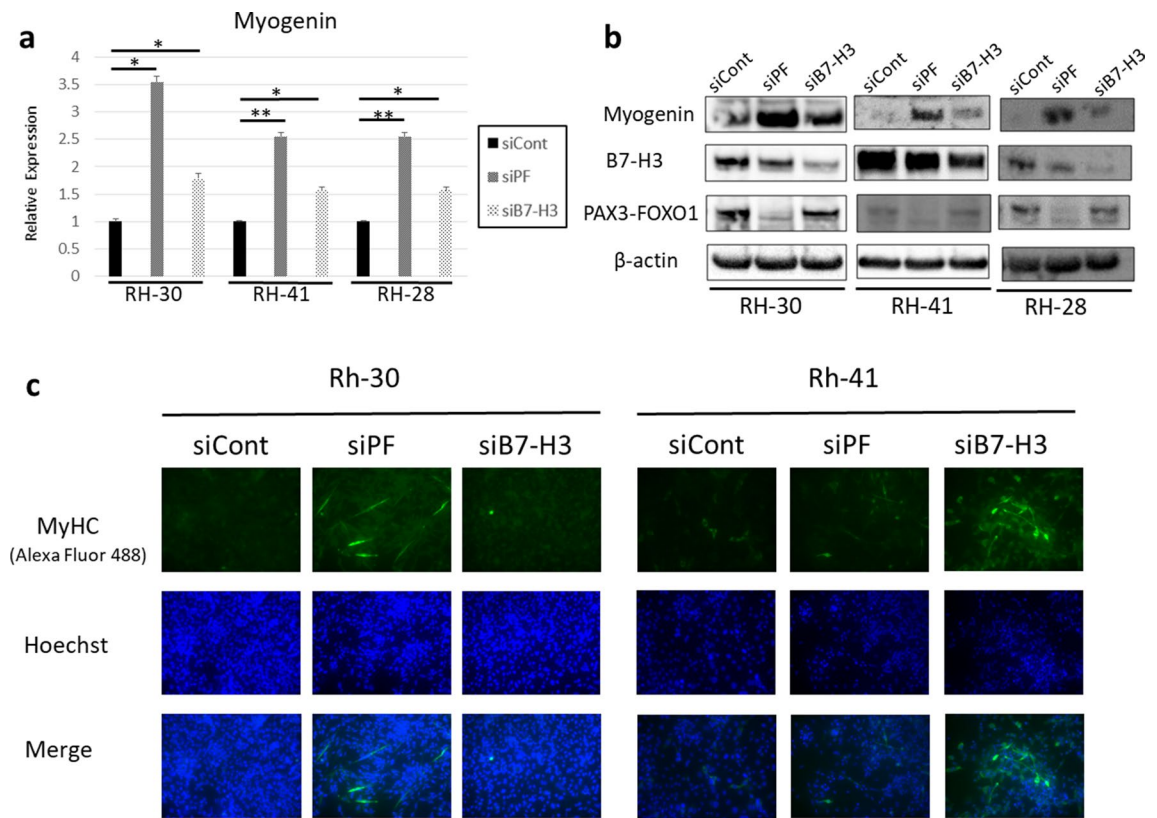


Figure 6. Knockdown of *PAX3-FOXO1* and *B7-H3* induces the expression of myogenin and may induce myoblast differentiation. (a) Quantitative real-time PCR analysis of *myogenin*. (b) Western blot analysis of myogenin. Knockdown of *PAX3-FOXO1* (detected by anti-PAX3 antibody) and *B7-H3* induces the expression of myogenin. (c) Immunofluorescence of myosin heavy chain. Results shown represent means \pm SD. * $p < 0.05$, ** $p < 0.01$, by two-tailed unpaired *t* test.

B7-H3-expressing relapsed or refractory malignant solid tumors, including ARMS, is currently being conducted (trial NCT02982941).

Our results demonstrate that *B7-H3* affects cell migration and myogenic differentiation and is one of the cancer driver genes in *PAX3-FOXO1* positive ARMS. As cancer antigen escape seems less likely to occur when the cancer driver gene is a target antigen, *B7-H3*-targeting immunotherapy might be an attractive treatment option for *PAX3-FOXO1* positive ARMS, although we did not examine the anti-*B7-H3* targeted therapy for ARMS in this study. The analysis of *B7-H3* targeted therapy is warranted in the future.

This study has several limitations. First, we did not investigate the association between *B7-H3* and tumor immunity in ARMS, although the GSEA indicated that gene sets related to $\text{INF-}\gamma$ production and T cell-mediated cytotoxicity were inactivated by knockdown of *PAX3-FOXO1* or *B7-H3*. As *B7-H3* is thought to be involved in tumor evasion from host immunity in other cancers, the relationship between *B7-H3* and tumor evasion should be a focus of future studies. Second, we used only one siRNA for each gene. Therefore, we could not exclude the possibility of off-target effect by siRNA. Third, we did not investigate the function of *B7-H3* in ARMS by in vivo experiments. In vivo experiments using the siRNA-treated cells would provide more evidence that strengthen our study results.

In conclusion, our findings demonstrate that *PAX3-FOXO1* regulates *B7-H3* expression, and *PAX3-FOXO1* and *B7-H3* are commonly associated with multiple pathways related to an aggressive phenotype in ARMS. In particular, *PAX3-FOXO1* and *B7-H3* contribute to cell migration and inhibit myogenic differentiation. This study provides evidence that *B7-H3* contributes to the malignant characteristics of *PAX3-FOXO1* positive ARMS.

Materials and methods

Cell lines and cell culture. *PAX3-FOXO1* positive human ARMS cell lines, Rh-30, Rh-41, and Rh-28 that were kindly provided by Peter J. Houghton M (The Greehey Children's Cancer Research Institute, San Antonio, TX), as well as *PAX3-FOXO1* negative human ERMS cell line, RD that was obtained from JCRB (Japanese Collection of Research Bioresources) Cell Bank, were used in this study. The cells were maintained in RPMI 1640 medium (Nakarai Tesque, Kyoto, Japan), supplemented with 10% fetal bovine serum (FBS; Gibco, Carlsbad, CA), penicillin (100 U/mL), and streptomycin (100 $\mu\text{g/mL}$) at 37 $^{\circ}\text{C}$ in a humidified atmosphere of 5% CO_2 .

siRNA and knockdown. siCont and an siB7-H3 were purchased from Invitrogen (Carlsbad, CA; catalog numbers AM4611 and AM16708-s37290, respectively). siPF was custom-synthesized as described previously²⁶. Briefly, siPF targets the fusion sites between exon 7 of *PAX3* and exon 2 of *FOXO1*. The sense and antisense sequences for siPF were 5'-CCUCUCACCUCAGAAUUCAtt-3' and 5'-UGAAUUCUGAGGUGAGAGGtt-3', respectively. Transfection of cells with the siRNAs was carried out using Lipofectamine RNAiMAX (Invitrogen) according to the procedures recommended by the manufacturer. The final concentration of siRNAs was 5 nM. Six hours after transfection, the medium containing the siRNAs and Lipofectamine RNAiMAX was replaced with fresh RPMI1640 medium containing 10% FBS.

RNA extraction, reverse transcription, and qRT-PCR. Total RNA was extracted from rhabdomyosarcoma cell lines using an RNeasy mini kit (Qiagen, Hilden, Germany) according to the manufacturer's instructions. cDNA was synthesized using a SuperScript VILO cDNA synthesis kit (Invitrogen) according to the manufacturer's instructions. qRT-PCR was carried out in a 7300 Real time PCR System (Applied Biosystems, Carlsbad, CA) with TB Green Premix Ex Taq II (Clontech Laboratories, Madison, WI) according to the manufacturer's protocol. The PCR primers used in the study were as follows: for *GAPDH*: 5'-GCACCGTCAAGGCTGAGAC-3' (forward) and 5'-ATGGTGGTGAAGACGCCAGT-3' (reverse); for *PAX3-FOXO1*: 5'-TCCAACCCC ATGAACCCC-3' (forward) and 5'-GCCATTTGGAAAAGTGTGATCC-3' (reverse); for *B7-H3*: 5'-CAAGGC AATGCATCCCTGAG-3' (forward) and 5'-CTTCGAGTAGGGAGCGGC-3' (reverse); for *MYOG*: 5'-GGA CCGAGCTCACCTGA-3' (forward) and 5'-TTACACACCTTACACGCCCA-3' (reverse). The levels of target mRNAs were determined using the delta delta CT method and were normalized to the expression level of *GAPDH*. All experiments were performed in triplicate.

Western blot analysis. Twenty-four hours after transfection with siRNAs, the cells were lysed with RIPA buffer (Nakarai Tesque). Samples were boiled for 10 min in NuPAGE sample buffer (Invitrogen) and were separated by SDS-polyacrylamide gel electrophoresis. The proteins were subsequently transferred onto an Immobilon-P PVDF transfer membrane (Millipore, Bedford, MA). The membranes were blocked with 3% bovine albumin (Nakarai Tesque) prepared in phosphate-buffered saline with Tween 20 (PBS-T) and then incubated with one of the primary antibodies: β -actin (1:10,000, Sigma-Aldrich, St. Louis, MO), *PAX3* (1:500, R&D Systems, Minneapolis, MN), Myogenin (1:500, Novus Biologicals, Centennial, CO), and B7-H3 (1:1000, Cell Signaling Technology, Danvers, MA). The membranes were then washed with PBS-T and incubated with anti-mouse or anti-rabbit secondary antibody (1:10,000, Santa Cruz Biotechnology, Santa Cruz, CA). Antibody binding was detected using an ECL prime detection system (GE Healthcare, Buckinghamshire, UK).

Flow cytometry. Cells were harvested, washed twice with PBS, and incubated for 30 min on ice with PE-conjugated anti-human B7-H3 antibody (Biolegend, San Diego, CA). Next, the cells were analyzed on a FACS Calibur (BD Biosciences, Franklin Lakes, NJ) with the FlowJo software (Treestar, San Carlos, CA).

Gene expression analysis. Total RNA was extracted from RH-30 cells transfected with siCont, siPF, or siB7-H3. The total RNA was used for cRNA target synthesis using a GeneChip 3'IVT PLUS Reagent Kit (Thermo Fisher Scientific, Waltham, CA). Biotin-labeled cRNA was hybridized to a GeneChip Human Genome U133 Plus 2.0 Array (Thermo Fisher Scientific). Hybridized arrays were stained and scanned with a Genechip 3000 7G Scanner (Thermo Fisher Scientific). Data were analyzed with the Affymetrix Expression Console Software 1.4.1. All microarray data are available at the Gene Expression Omnibus database under accession number GSE127703. GSEA was performed using GSEA 3.0 (Broad Institute, San Diego, CA). A group consisting of RH-30-siPF and RH-30-siB7-H3 was compared with RH-30-siCont, and gene sets at a nominal p value (NOM p -val) < 5% were considered to be significantly enriched.

Wound healing assay. After transfection of cells with siRNAs, the cell layers were scratched using a pipette tip. Immediately after scratching (0 h), the plates were photographed and the wound area was measured using the ImageJ software and defined as the original area (100%). After 24 h of scratching, the plates were photographed again. In addition, the area of the healed wound was measured and presented as a percentage of the original area. All assays were performed in triplicate.

Transwell migration assay. At 24 h of transfection of cells with the siRNAs, each cell line was resuspended in serum-free RPMI medium. Twenty-four well-sized transwell plates with an 8- μ m pore size (Corning, Corning, NY) were used for this assay. First, 1.0×10^5 cells suspended in 100 μ L of serum-free medium were seeded on each insert, and 650 μ L of RPMI medium with 10% FBS was added to the receiver plates. The plates were incubated for 24 h, and cells migrating onto the receiver plates were quantified as relative light units (RLU) using the Cell Titer Glo luminescent cell viability assay (Promega, Heidelberg, Germany) according to the procedures recommended by the manufacturer. All the assays were performed in triplicate.

Immunofluorescence. At 24 h of transfection of cells with the siRNAs, Rh-30 and Rh-41 cells were resuspended in serum-free RPMI medium. After 7 days of resuspension, cells were fixed with 4% paraformaldehyde and permeabilized with 0.1% Triton-X100. Next, the cells were washed and incubated with anti-MyHC antibody (Sigma-Aldrich) overnight (1:350), rinsed with PBS, and incubated with Alexa Fluor 488 goat anti-mouse IgG (Life Technologies, Carlsbad, CA) for 1 h (1:200). Nucleic acids were stained with Hoechst, using the NucBlue

Live Cell Stain Ready Probes Reagent (Invitrogen). A BZ-X800 confocal microscope (KEYENCE, Osaka, Japan) was used for observation.

Statistical analysis. The results are shown as mean \pm SD of three independent experiments. Statistical analysis was performed using the two-tailed Student's *t* test. A *p* value < 0.05 was considered statistically significant.

Received: 25 April 2021; Accepted: 7 September 2021

Published online: 22 September 2021

References

1. Chapoval, A. I. *et al.* B7-H3: A costimulatory molecule for T cell activation and IFN- γ production. *Nat. Immunol.* **2**, 269–274 (2001).
2. Luo, L. *et al.* B7-H3 enhances tumor immunity in vivo by costimulating rapid clonal expansion of antigen-specific CD8⁺ cytolytic T cells. *J. Immunol.* **173**, 5445–5450 (2004).
3. Prasad, D. V. *et al.* Murine B7-H3 is a negative regulator of T cells. *J. Immunol.* **173**, 2500–2506 (2004).
4. Suh, W. K. *et al.* The B7 family member B7-H3 preferentially down-regulates T helper type 1-mediated immune responses. *Nat. Immunol.* **4**, 899–906 (2003).
5. Castriconi, R. *et al.* Identification of 4Ig-B7-H3 as a neuroblastoma-associated molecule that exerts a protective role from an NK cell-mediated lysis. *Proc. Natl. Acad. Sci. U S A.* **101**, 12640–12645 (2004).
6. Crispen, P. L. *et al.* Tumor cell and tumor vasculature expression of B7-H3 predict survival in clear cell renal cell carcinoma. *Clin. Cancer Res.* **14**, 5150–5157 (2008).
7. Inamura, K. *et al.* Tumor B7-H3 (CD276) expression and smoking history in relation to lung adenocarcinoma prognosis. *Lung Cancer* **103**, 44–51 (2017).
8. Loos, M. *et al.* Expression of the costimulatory molecule B7-H3 is associated with prolonged survival in human pancreatic cancer. *BMC Cancer* **9**, 463 (2009).
9. Wang, L. *et al.* B7-H3 is overexpressed in patients suffering osteosarcoma and associated with tumor aggressiveness and metastasis. *PLoS ONE* **8**, e70689. <https://doi.org/10.1371/journal.pone.0070689> (2013).
10. Majzner, R. G. *et al.* CAR T Cells targeting B7-H3, a pan-cancer antigen, demonstrate potent preclinical activity against pediatric solid tumors and brain tumors. *Clin. Cancer Res.* **25**, 2560–2574 (2019).
11. Loo, D. *et al.* Development of an Fc-enhanced anti-B7-H3 monoclonal antibody with potent antitumor activity. *Clin. Cancer Res.* **18**, 3834–3845 (2012).
12. Du, H. *et al.* Antitumor responses in the absence of toxicity in solid tumors by targeting B7-H3 via chimeric antigen receptor T Cells. *Cancer Cell* **35**, 221–237 (2019).
13. Chen, L. *et al.* B7-H3 expression associates with tumor invasion and patient's poor survival in human esophageal cancer. *Am. J. Transl. Res.* **7**, 2646–2660 (2015).
14. Jiang, B. *et al.* The co-stimulatory molecule B7-H3 promotes the epithelial-mesenchymal transition in colorectal cancer. *Oncotarget* **7**, 31755–31771 (2016).
15. Li, Y. *et al.* B7-H3 promotes the migration and invasion of human bladder cancer cells via the PI3K/Akt/STAT3 signaling pathway. *J. Cancer.* **8**, 816–824 (2017).
16. Li, Y. *et al.* B7-H3 promotes gastric cancer cell migration and invasion. *Oncotarget* **8**, 71725–71735 (2017).
17. Lim, S. *et al.* Immunoregulatory protein B7-H3 reprograms glucose metabolism in cancer cells by ROS-mediated stabilization of HIF1 α . *Cancer Res.* **76**, 2231–2242 (2016).
18. Lin, L. *et al.* B7-H3 promotes multiple myeloma cell survival and proliferation by ROS-dependent activation of Src/STAT3 and c-Cbl-mediated degradation of SOCS3. *Leukemia* **33**, 1475–1486 (2018).
19. Mesri, M. *et al.* Identification and characterization of angiogenesis targets through proteomic profiling of endothelial cells in human cancer tissues. *PLoS ONE* **8**, e78885. <https://doi.org/10.1371/journal.pone.0078885> (2013).
20. Kramer, S., Meadows, A. T., Jarrett, P. & Evans, A. E. Incidence of childhood cancer: Experience of a decade in a population-based registry. *J. Natl. Cancer Inst.* **70**, 49–55 (1983).
21. Barr, F. G. *et al.* Rearrangement of the PAX3 paired box gene in the paediatric solid tumour alveolar rhabdomyosarcoma. *Nat. Genet.* **3**, 113–117 (1993).
22. Barr, F. G. *et al.* In vivo amplification of the PAX3-FKHR and PAX7-FKHR fusion genes in alveolar rhabdomyosarcoma. *Hum. Mol. Genet.* **5**, 15–21 (1996).
23. Galili, N. *et al.* Fusion of a fork head domain gene to PAX3 in the solid tumour alveolar rhabdomyosarcoma. *Nat. Genet.* **5**, 230–235 (1993).
24. Sorensen, P. H. *et al.* PAX3-FKHR and PAX7-FKHR gene fusions are prognostic indicators in alveolar rhabdomyosarcoma: A report from the children's oncology group. *J. Clin. Oncol.* **20**, 2672–2679 (2002).
25. Cao, L. *et al.* Genome-wide identification of PAX3-FKHR binding sites in rhabdomyosarcoma reveals candidate target genes important for development and cancer. *Cancer Res.* **70**, 6497–6508 (2010).
26. Kikuchi, K. *et al.* Effects of PAX3-FKHR on malignant phenotypes in alveolar rhabdomyosarcoma. *Biochem. Biophys. Res. Commun.* **365**, 568–574 (2008).
27. Zhang, L. & Wang, C. Identification of a new class of PAX3-FKHR target promoters: A role of the Pax3 paired box DNA binding domain. *Oncogene* **26**, 1595–1605 (2007).
28. Kang, F. B. *et al.* B7-H3 promotes aggression and invasion of hepatocellular carcinoma by targeting epithelial-to-mesenchymal transition via JAK2/STAT3/Slug signaling pathway. *Cancer Cell Int.* **15**, 45. <https://doi.org/10.1186/s12935-015-0195-z> (2015).
29. Tekle, C. *et al.* B7-H3 contributes to the metastatic capacity of melanoma cells by modulation of known metastasis-associated genes. *Int. J. Cancer* **130**, 2282–2290. <https://doi.org/10.1002/ijc.26238> (2012).
30. Libura, J. *et al.* CXCR4-SDF-1 signaling is active in rhabdomyosarcoma cells and regulates locomotion, chemotaxis, and adhesion. *Blood* **100**, 2597–2606 (2002).
31. Kashima, K. *et al.* Inhibition of metastasis of rhabdomyosarcoma by a novel neutralizing antibody to CXC chemokine receptor-4. *Cancer Sci.* **105**, 1343–1350 (2014).
32. Chen, L. *et al.* Aberrant expression of STYK1 and E-cadherin confer a poor prognosis for pancreatic cancer patients. *Oncotarget* **8**, 111333–111345 (2017).
33. Shi, Y., Zhang, J., Liu, M., Huang, Y. & Yin, L. SMAD3 inducing the transcription of STYK1 to promote the EMT process and improve the tolerance of ovarian carcinoma cells to paclitaxel. *J. Cell. Biochem.* **120**, 10796–10811 (2019).
34. Wright, W. E., Sassoon, D. A. & Lin, V. K. Myogenin, a factor regulating myogenesis, has a domain homologous to MyoD. *Cell* **56**, 607–617 (1989).

35. Walters, Z. S. *et al.* JARID2 is a direct target of the PAX3-FOXO1 fusion protein and inhibits myogenic differentiation of rhabdomyosarcoma cells. *Oncogene* **33**, 1148–1157 (2014).
36. Picarda, E., Ohaegbulam, K. C. & Zang, X. Molecular pathways: targeting B7-H3 (CD276) for human cancer immunotherapy. *Clin. Cancer Res.* **22**, 3425–3431 (2016).
37. Seaman, S. *et al.* Eradication of tumors through simultaneous ablation of CD276/B7-H3-positive tumor cells and tumor vasculature. *Cancer Cell* **31**, 501–515 (2017).
38. Souweidane, M. M. *et al.* Convection-enhanced delivery for diffuse intrinsic pontine glioma: A single-centre, dose-escalation, phase 1 trial. *Lancet. Oncol.* **19**, 1040–1050 (2018).

Acknowledgements

We would like to thank Editage (www.editage.jp) for English language editing.

Author contributions

M.M. designed the study. T.K. and Y.S. contributed to the data collection. All authors contributed to the analysis and interpretation of the data. T.K. and M.M. drafted the manuscript. All authors critically reviewed and approved the final version of the manuscript.

Funding

The present study was supported by JSPS KAKENHI Grant-in-Aid for Scientific Research (C) [grant number 16K10036].

Competing interests

The authors declare no competing interests.

Additional information

Supplementary Information The online version contains supplementary material available at <https://doi.org/10.1038/s41598-021-98322-z>.

Correspondence and requests for materials should be addressed to M.M.

Reprints and permissions information is available at www.nature.com/reprints.

Publisher's note Springer Nature remains neutral with regard to jurisdictional claims in published maps and institutional affiliations.



Open Access This article is licensed under a Creative Commons Attribution 4.0 International License, which permits use, sharing, adaptation, distribution and reproduction in any medium or format, as long as you give appropriate credit to the original author(s) and the source, provide a link to the Creative Commons licence, and indicate if changes were made. The images or other third party material in this article are included in the article's Creative Commons licence, unless indicated otherwise in a credit line to the material. If material is not included in the article's Creative Commons licence and your intended use is not permitted by statutory regulation or exceeds the permitted use, you will need to obtain permission directly from the copyright holder. To view a copy of this licence, visit <http://creativecommons.org/licenses/by/4.0/>.

© The Author(s) 2021